Design and Optimization of Brushless DC Motor for Electric Boat Thruster

Dewi Rianti Mandasari
Research Center for Process and Manufacturing Industry Technology, National Research and Innovation Agency of Republic Indonesia

Yulianto, Katri
Research Center for Process and Manufacturing Industry Technology, National Research and Innovation Agency of Republic Indonesia

Amelia, Lia
Research Center for Process and Manufacturing Industry Technology, National Research and Innovation Agency of Republic Indonesia

Aziz, Amiruddin
Research Center for Process and Manufacturing Industry Technology, National Research and Innovation Agency of Republic Indonesia

他

https://doi.org/10.5109/7151773

出版情報：Evergreen. 10 (3), pp.1928-1937, 2023-09. 九州大学グリーンテクノロジー研究教育センター
バージョン：

Design and Optimization of Brushless DC Motor for Electric Boat Thruster

Dewi Rianti Mandasari[1,*], Katri Yulianto[1], Lia Amelia[1], Amiruddin Aziz[1], Endra Dwi Purnomo[1], Faisal[1], Cuk Supriyadi Ali Nandar[2]

[1]Research Center for Process and Manufacturing Industry Technology,
National Research and Innovation Agency of Republic Indonesia, DKI Jakarta, Indonesia.

[2]Research Center for Energy Conversion and Conservation,
National Research and Innovation Agency of Republic Indonesia, DKI Jakarta, Indonesia.

*Author to whom correspondence should be addressed:
E-mail: dewi031@brin.go.id

(Received May 2, 2023; Revised July 6, 2023; accepted September 17, 2023).

Abstract: This research provided a detailed examination, which was used to develop a Brushless Direct Current (BLDC) motor for Indonesia's Electric Boat Conversion Program, specifically focusing on reducing cogging torque. Several approaches, including stator skewing, were examined while considering manufacturing complexities and costs. A novel methodology was used to determine the optimal skew angle, considering the limitations of allowable cogging torque, which was set at 10% of the rated torque based on prior research and the manufacturing process. The result showed that a skew angle of 6° outperformed empirical calculations at 15°. Mechanical evaluations also showed that the natural frequency remained within acceptable limits at the 6° skew angle. Therefore, a skew angle of 6° was recommended for the 10 kW BLDC motor used in electric boat applications. This research contributed to advancing motor design for electric boat conversions, effectively balancing performance optimization with manufacturing feasibility.

Keywords: electric boat; BLDC motor; cogging torque; skewing stator; optimization; manufacture

1. Introduction

Climate change is one of the most significant threats the world is currently confronting. It is primarily driven by the increase in greenhouse gases resulting from global warming and contributing to the depletion of the ozone layer. The concentration of these gases in the troposphere is rising, largely due to human-made activities such as electricity production, industrialization, and transportation[1)]. Recent assessments from the International Energy Agency revealed that approximately 25% of global CO2 emissions could be attributed to the transportation industry[2,3)]. Consequently, nations worldwide, including Indonesia, strive to reduce gas emissions from the transportation industry[4)].

Indonesia's topography, characterized by numerous islands and rivers, heavily relies on boats for transportation, specifically in coastal and remote areas. Among the various types of water transportation, small and medium-sized boats are the most prevalent, serving multiple purposes such as passenger commuting, fishing, cargo transport, and recreational activities[5)]. Unfortunately, most of these boats in Indonesia are currently powered by Internal Combustion Engines (ICE) running on diesel fuel. This dependence on diesel engines leads to carbon dioxide (CO_2) and nitrogen oxides NO_x emissions, which contribute to air pollution and the accumulation of greenhouse gases, further exacerbating global warming. Given that port emissions are closely tied to fuel emissions, it becomes crucial to assess and address the environmental impact of each port, promoting the adoption of efficient and sustainable practices to reduce emissions in Indonesia[6)]. Numerous research proposed converting the ICE into an electric propulsion system linked to an electric machine (EM) powered by batteries[5)].

The Indonesian government has implemented an electric vehicle program to reduce the effect of greenhouse gas emissions while accelerating the development of the domestic electric vehicle industry. This program aims to leverage technological advancements to introduce Electric Boat (E-Boat) into the market of electric vehicles. The electric propulsion system of a boat typically consists of components such as an electric motor, transmission systems, power converters, electrical energy generation systems, storage systems, and propellers[7)]. While the electric motor used in E-Boats differs from that in

conventional electric vehicles, it commonly employs a Brushless DC (BLDC) motor. According to preliminary research, BLDC motors offer high efficiency and power density, resulting in improved battery life for a given size. These characteristics make BLDC motors particularly well-suited for electric propulsion applications in boats[7].

The presence of a permanent magnet (PM) in the rotor of a BLDC motor gives rise to cogging torque due to magnetic interactions between the rotor and stator[8]. In slot motors, the air gap flux density experiences fluctuations caused by variations in permeance along the air gap, resulting from interactions between the stator teeth, slots, and rotor. These fluctuations lead to the generation of harmonic components in addition to the fundamental air gap flux density, contributing to torque ripple. Cogging torque is present under conditions of high load and low speed when the inertia of the system is unable to smooth out the output torque effectively. Consequently, this results in significant output torque ripple, which can induce noise and cause the motor to run roughly[9].

Numerous research has been conducted to address cogging torque in BLDC motors, and two main approaches have been identified. One method involves redesigning the motor by optimizing the skew angle on either the stator or rotor core. The other approach focuses on increasing the air gap between the rotor and stator. Past investigations specifically targeted cogging torque reduction in BLDC interior permanent magnet (IPM) V-shape type motors for electric vehicle applications, and these methods have demonstrated their effectiveness. The results showed that optimizing the BLDC IPM motor to reduce cogging torque yields remarkable results, specifically when utilizing a skew angle on the stator core or, in certain cases, on the rotor core, alongside enlarging the air gap. A skew angle on the stator core can reduce almost the total of the cogging torque[10].

Skewing refers to the process of twisting the rotor or stator of a machine in a helical pattern[11]. Theoretically, fabricating a skew angle on the stator core is relatively straightforward, as the thin steel laminations can be twisted before stacked and glued. However, achieving the desired skew angle in practice can be challenging. The cosine effect of the skew angle on the stator leads to a reduction in the cross-sectional area of the stator slots and an elongation of the wire within the slot, resulting in increased copper losses[11]. It is crucial to determine an appropriate skew angle, as skewing the slot help minimize torque ripple, reduce the average torque and impact dynamic performance in both positive and negative directions[12].

When optimizing the skew angle on the stator, it is essential to consider factors such as high efficiency, ease of manufacturing, and production cost. Manufacturing BLDC motors with a stator skew in Indonesia poses unique challenges, making it a novel approach for the country's electric motor production. Differing from other research that focuses only on eliminating cogging torque in BLDC motors, this research also considers the manufacturing difficulties capable of complicating local industries producing the motor.

The primary focus of this research is to investigate the impact of varying or optimizing the skew angle on the reduction of cogging torque, motor complexity, and manufacturing ease in the production of high-performance and efficient BLDC electric motors. The Finite Element Analysis (FEA) method was used in this research, with simulations conducted using Ansys Maxwell software, specifically targeting a 10 kW motor.

According to the research by F. S. Bahrim et al.[13], the maximum cogging torque should not exceed 10% of the average torque because it can lead to undesirable high vibration and noise levels. Ion Boldea[14] stated that the cogging torque less than 10% of the rated torque, can be further reduced for general purposes. Based on these findings, a maximum limit of 10% of the rated torque has been established for the cogging torque.

The organization of this research is as follows: Section II, titled "Methodology," started by examining the propulsion system requirements of the boat and selecting the suitable specifications for the BLDC motor to meet the desired performance of the E-Boat propulsion system. This section also explained the cogging torque, the harmonics and the back EMF of the BLDC motor.

This research is structured as follows: Section 2 addressed the boat propulsion system requirements and subsequently determined the appropriate specifications for the BLDC motor that can fulfil these requirements. Section 3 analyzed the motor performance, encompassing a detailed explanation of cogging torque, harmonics, and the back EMF of a BLDC motor. Additionally, the section presented the methodology used to validate the motor design using a motor design model. Section 4 comprehensively compared motor performance across various skew angle stators. Section 5 is dedicated to the conclusion of this research.

2. BLDC Motor Design and Requirements

In contrast to land vehicles, boat propulsion motors face unique challenges, such as exposure to seawater and high humidity. These motors operate at high speeds and are typically installed with limited battery capacity within a predetermined casing size and propeller configuration. Table 1 shows the requirements for an electric motor for boat propulsion.

Table 1. The design requirement for an electric boat thruster

Parameter	Value	Unit
Battery Voltage	60	VDC
Rated Power	10	kW
Speed of Motor	2500	rpm
Rated Torque	38.2	Nm

This research used a BLDC IPM motor V-shape type for E-Boat propulsion. The motor selection is based on previous research, demonstrating its widespread use in electric vehicle applications due to its ease of maintenance, high power density, reliability, and efficiency[15–17]. Commercially, manufacturers and suppliers often opt for permanent magnet-assisted synchronous reluctance motors (PMaSynRM) or interior permanent magnet (IPM) motors for their electric traction motors, primarily due to their high efficiency and torque characteristics[18]. A high-efficiency motor with controllable high torque and speed is important for the electric vehicle market in Indonesia[19]. Compared to permanent surface magnet (SPM) motors, IPM motors can gather more magnetism due to their large saliency ratio, thereby causing additional reluctant torque on original magnetic torque, leading to higher torque density. Almost all PM motors use the radial flux selection because the manufacturing process is firmly established, simple and allows electrical loading to be optimized through slots[20]. PM in this motor is designed in a V-shape to enhance PM excitation further. This shape is specifically selected to meet the requirements of withstanding saltwater and high humidity conditions, which are typical challenges faced in marine applications. Table 2 shows the detailed specifications of the BLDC motor, designed to fulfil the specific system requirements.

Table 2. Specification of BLDC motor

Parameter	Value	Unit
Type	BLDC IPM V-shape	-
Rated Power	10	kW
Voltage	60	VDC
Speed	2500	rpm
Torque	38.2	Nm
Poles	8	-
Air Gap	0.6	mm
Stator Outer Diameter	175	mm
Lamination Length	105	mm
Stator Slots	12	-
Rotor Outer Diameter	98.80	mm
Magnet Type	NdFe52	-
Magnet Thickness	3	mm
Magnet Width	14.30	mm
Number of Segment Magnet	2	pcs

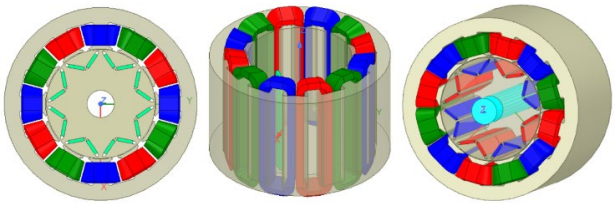

Fig. 1: The preliminary design of the BLDC motor

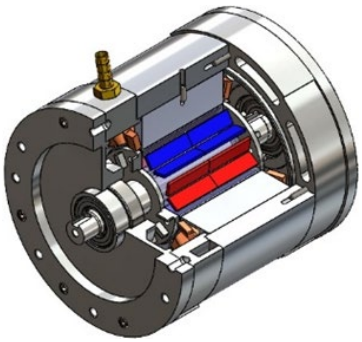

Fig. 2: 3D design of electric boat thruster.

The BLDC motor is developed using two segment magnets at the rotor core. According to preliminary research, several reasons exist for adopting segmented PM. For instance, the carrier harmonics generated by the inverter play a critical role in causing a substantial portion of the magnet eddy current losses in motors with distributed windings. This is because the high-frequency harmonic eddy currents amplify the skin effect induced by the carrier harmonics[21]. The eddy current losses can be reduced by segmenting PM[21–23]. Dutta et al. n.d. stated that segmenting PM reduced the cogging torque, although it was not too significant[24]. Duan et al. and Gu et al. proved that segmented IPMSM improved field weakening capability due to higher d-axis inductance and reduced PM flux linkage. This enhancement contributed to the improved anti-demagnetization capability of PM and decreased air gap flux, which improved the overall motor performance[25,26].

Generally, the BLDC motor produced three types of torque, namely mutual, reluctance, and cogging. The cogging torque resulted from the interaction between PM embedded in the rotor and the slots in the stator, which is inherent in BLDC motors with IPM V-shape. The torque ripple was caused by the cogging torque produced due to this interaction, which led to noise and shaft vibration making the motor to run smoothly, particularly at low speeds and with light loads[9].

3. Motor Performance Analysis

3.1 Cogging torque analysis

The cogging torque was determined by aligning the rotor magnets with the teeth or stator poles, independent of current flow. The maximum cogging occurred when the interpolar axis was aligned with the end side of the stator, which led to the greatest change in magnetic energy[27]. Common research used as assumptions regarding torque

on motors with PM include[28]:

- The amount of magnetic energy is determined by the number of PM and their placement in the air gap.
- The vacuum permeability equals the sum of the PMs and air permeability.
- The permeability of the iron is considered indefinite, and
- The air gap's flux density remains consistent in the radial direction.

The following equation represents the cogging torque:

$$T_{cog} = -\frac{1}{2}\,\emptyset^2\,\frac{dR}{d\theta} \tag{1}$$

$\emptyset$ denotes the magnetic flux that traverses the air gap, and R is the total reluctance traversed by the flux. When, according to (1), the reluctance of the rotor fails to change while rotating, the cogging torque becomes zero. This is because the magnet flux set is squared, while the cogging torque is independent of the flux direction[29].

The energy method describes the cogging torque of the electric machine. The equation for magnetic co-energy (W) related to the movable displacement component (ϑ_r) is used to derive torque[30]:

$$T_{cog}(\vartheta_r) = -\frac{\partial W}{\partial \vartheta_r} \tag{2}$$

The magnetic energy (W) is explained based on the assumptions in equation (3):

$$W = \frac{1}{2\mu_0}\int_{V_g} B^2 dV \tag{3}$$

Where B denotes the flux density of the air gap under zero load conditions, and μ_0 represents the vacuum permeability, influenced by the magnetic energy and volume of the air gap (V_g)[31]. The techniques used to minimize cogging torque through stator slot design involve various approaches, such as eliminating slots, using skewed or uniquely shaped slots, and carefully selecting the number of slots and poles. The cogging torque can be reduced through good design[32].

Skewing the slots on the stator core is a relatively straightforward process that can be conducted during the construction of the motor by skewing the stator before stacking and glueing. The stator was intentionally skewed to reduce cogging torque in this research. According to reference (3), the magnetic energy, which significantly influences cogging torque, was distributed uniformly across the air gap. Therefore, the torque value on skew angle can be explained by equation (4) using the periodicity feature[8].

$$T_{skew}(\theta) = \sum_{i=1}^{\infty} K_{sk} T_i \sin\left(iC_p\theta_m + \theta_i\right) \tag{4}$$

The skew factor is shown in K_{sk}, T_i represents the absolute value of the harmonic content, while C_p is the lowest common multiple of the number of stator slots and poles. When the motor is in motion, θ_m is the mechanical angle between the stator and rotor axis, and θ_i denotes the phase angle of K_{sk}. The value of K_{sk} is equal to 1, assuming the motor laminations are not skewed. The skew factor is explained in equation (5).

$$K_{sk} = \frac{\sin(i\,C_p\pi\alpha_{sk}/N_s)}{i\,\frac{C_p\pi\alpha_{sk}}{N_s}} \quad i = 1,2,3,\ldots \tag{5}$$

The number of slots and skew angle is denoted with N_s and α_{sk}, which can be determined using Equation (6).

$$\alpha_{sk} = \frac{360^0}{N_s N_{period}} \tag{6}$$

N_{period} expresses the cogging torque period in a single slot pitch. The relationship between N_{period} and the optimal skew angle to minimize cogging torque is shown in equation (7). HCF is the largest shared divisor between the number of poles and stator slot number:

$$N_{period} = \frac{N_p}{HCF(N_{s,}N_p)} \tag{7}$$

Using Equations (6) and (7), the skew angle for the BLDC motor with 12 stator slots and 8 poles is 15^0, which successfully reduced the cogging torque by approximately 100%.

3.2 Harmonic analysis

Certain combinations of slots and poles produce spatial harmonics with a high frequency. These harmonics create rotating fields with different speeds and directions, leading to undesirable effects such as iron loss, eddy currents, vibrations, and noise. Harmonic fields rotate at varying speeds and directions, creating unwanted side effects such as eddy currents, iron loss, vibration, and noise. By skewing the stator windings, these harmonic fields can be reduced without altering the geometry of the stator slots. For the purpose of illustrating the influence of winding skew and stator skew angle, a full-pitch concentrated winding with N_k turns per coil is studied, where N_k was expressed as follows (8).

$$N_k = N_{t,}K_{pk}\,K_{dk}\,K_{sk} \tag{8}$$

Where $N_t, K_{dk}, K_{pk}, and\ K_{sk}$ denote the total number of turns within each coil, factors of harmonic distribution, harmonic pitch, and harmonic skew. The optimal skew angle in this method was determined by minimizing cogging torque and the machine's harmonic. The skew angle on the prototype was used to consider the manufacturing industry's capabilities.

3.3 Back EMF analysis

Magnetic flux produces back Electro-Motive Force (EMF) in stator coils. As the rotor turns, the coils generate a magnetic field, thereby inducing current, which is calculated using Faraday's, as shown in Equation (9)[8].

$$E\ (\theta) = \ -N\frac{d\phi(\theta)}{dt} = -N\omega\frac{d\phi(\theta)}{dt} \qquad (9)$$

Where N represents the number of rotations, ω denotes the angular velocity, and $\phi(\theta)$ represents the tooth flux. Equation (10) is used to calculate the Fourier transform of the flux, where ϕ_i denotes the values of the harmonic coefficients and θ_s is the angular slot pitch. The skew impact for flux in the k[th] tooth is $K_{sk\ /\ 2}$[8].

$$\phi_k(\theta) = \sum_{i=1}^{\infty} \phi_i\, K_{sk\ /\ 2}\ cos\left[\left(iN_p\theta - k\theta_s\right)/2\right] k \qquad (10)$$
$$= 0,1,..N_s - 1$$

The EMF harmonics can be determined by describing the harmonic components of the flux as shown in Equation (11).

$$E\ (\theta) = -N\omega\frac{N_p}{2}\sum_{i=1}^{\infty} \phi_i\, K_{sk\ /\ 2}\ cos\left[\left(iN_p\theta - k\theta_s\right)/2\right] \qquad (11)$$

3.4 Natural frequency analysis

Cogging torque analysis and EMF calculation methods based on Maxwell flux are commonly used to analyze cogging torque. Another effective analysis method is modal analysis, which considers the structural impact of different skew angles on the natural frequency. This is because the geometry and angle variations in the stator directly influence the volume and shape of the stator.

Modal analysis was performed through finite element analysis, providing insights into the structural vibration of the electric motor model. It enabled the determination of natural frequencies for each model type, incorporating the results from the electrical analysis. This information served as a guide for optimizing the motor design to reduce noise and vibration[33]. Ishibashi F. et al.[34], in their experimental analysis, showed that the natural frequency gradually decreased with a more complex ring shape in the induction motor, emphasizing the importance of natural frequency in developing quieter motors [34].

The vibration mode was calculated by equation (12) based on the natural frequency of undamped vibrations. M denotes the mass, and K represents stiffness. Therefore, the modal displacement vector was expressed as ϕ_i.

$$([K] - \omega_i{}^2[M])\{\phi_i\} = 0 \qquad (12)$$

The natural frequency (f_i) was determined using Equation (13):

$$f_i = \frac{\omega_i}{2\pi} \qquad (13)$$

3.5 Finite element analysis

In this research examined the impact of varying stator skew angles on cogging torque reduction, harmonics, back electromotive force (EMF), and vibration. The analysis evaluated the torque performance, losses, and motor efficiency. The simulation utilized ANSYS Maxwell, which combined the features of 3D Maxwell, 2D Maxwell, and RMXPRT to validate the design of an E-Boat thruster. The simulation involved using ANSYS to study the vibration effects of different skew angles on the stator core.

The ANSYS Mechanical was used to simulate the vibration effect of the skew angle on the stator core. This analysis helped evaluate the vibrational performance and frequency (Hz) of skewness in conjunction with cogging torque data obtained from the electrical analysis. Modal analysis techniques are employed to predict noise reduction[35]. When component signals are related to modes, their peak frequencies are closely aligned with those of the modal. However, when correlated with residual noise, their peak frequencies occasionally deviate from those of the modal. A simulation based on a frequency trend research[36] revealed a contrasting relationship between the natural frequency trend and noise levels. It became evident from both metrics that lower natural frequency values are inversely proportional to the noise levels.

4. Performance Comparison

4.1 Result of simulation

The results of the preliminary design of the BLDC motor indicated an ample cogging torque and torque ripple, as shown in Table 3.

Table 3. Simulation Result

Parameter	Value	Unit
Speed	2500	rpm
Output Power	10	kW
Shaft Torque	38.207	Nm
Maximum Torque	39.654	Nm
Cogging Torque	5.6615	Nm
Torque Ripple	9.3617	%
Efficiency	94.545	%

The simulation results of the BLDC motor met the desired performance requirements. However, there is a concern regarding the high cogging torque and torque ripple, which can cause vibration and potentially damage the motor. One way to address this issue was to introduce a skew angle to the stator core. By applying equation (2), the optimal stator skew angle was determined. In the case

of an 8-pole and 12-stator slot BLDC motor configuration, the calculated optimal angle was 15°. The larger the skew angle, the more complex the motor manufacturing process, hence, the need to optimize the process by reducing the angle of the stator skew to minimize the cogging torque. The maximum value for the skew angle depends on the angular distance between the magnet pole pitch and the angular distance between two adjacent magnets. The optimization process involved varying the stator skew angle from 0° to 15° at 0, 3, 6, 9, 12, and 15 angles. Additionally, a limit of 10% of the total torque was set as the cogging torque threshold, ensuring compliance with the motor design performance. This limit was determined based on the angular spacing of the magnet pole pitch and the impact of the angular separation between adjacent magnets on the motor performance. The configuration of the stator skew angle on a BLDC motor in ANSYS Maxwell is shown in Fig. 3.

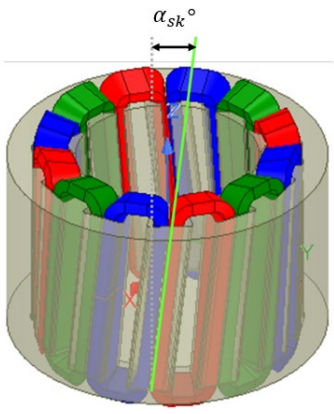

$\alpha_{sk} = 3n^{0}, n: 0,1,2,3,4,5$

Fig. 3: Various stator skew angle in ANSYS Maxwell 3D design.

The result of various skew angles is explained as follows.

4.2 Cogging Torque

The cogging torque graphic of the motor for various skew angles is shown in Fig. 4, indicating that without skewing on the stator, the cogging torque value was high, thereby leading to vibration and high noise[11]. The motor exhibits reduced cogging torque even with a small skew angle of 3°, resulting in decreased vibration and noise levels compared to the non-skewed motor. As the skew angle increased to 6°, 9°, 12°, and 15°, the cogging torque continued to decrease, eventually reaching the minimum performance torque target. Even though some cogging torque remains present, it falls within the predetermined limit of 10% of the total torque. For a 6° stator skew angle, the cogging torque measured 3.2 Nm, meeting the predefined limit and exhibiting a 42% reduction from the initial cogging torque. The 15° skew angle achieved a nearly 100% reduction in cogging torque, resulting in a smooth and noise-free motor operation, manufacturing complexity increased with a large skew angle. The motor performance target, ease of manufacture, and production cost, skewing the motor stator at 6° are considered the best choice.

Table 4. Cogging torque simulation results in different skew angle

Parameter	Skew Angle					
	0°	3°	6°	9°	12°	15°
Cogging Torque (Nm)	5.6615	4.3889	3.0196	1.8825	0.9195	0

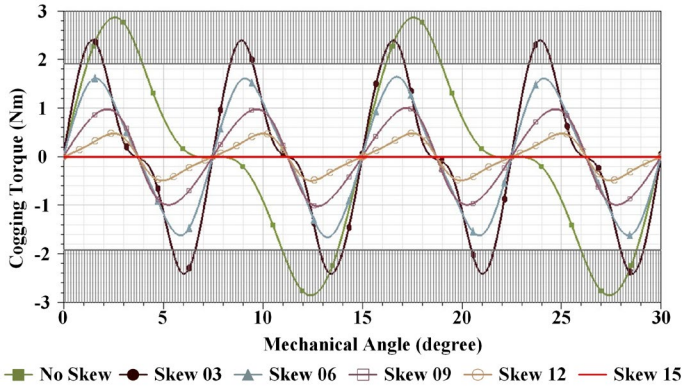

Fig. 4: Cogging torque graphic.

4.3 Back EMF

Back EMF is produced by the rate of change of the flux linkage of a coil regarding time. Fig. 5 shows the back EMF graph of the motor at various skew angles. The BLDC motor back EMF is closely associated with the pulsating torque and significantly influences the overall performance of the machine. The ideal condition of back EMF is a trapezoidal waveform[37]. In Fig. 5, the graphic showed a smoother and more trapezoidal waveform when the skew angle increased, affecting motor performance. At the 6° stator skew angle, the back EMF waveform was smooth and more trapezoidal, which is enough to increase the motor performance.

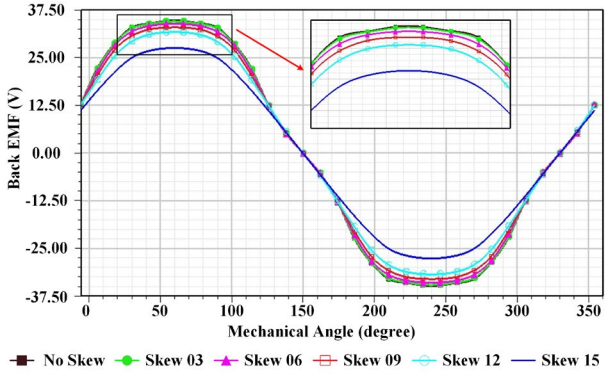

Fig. 5: Back EMF BLDC motor graphic.

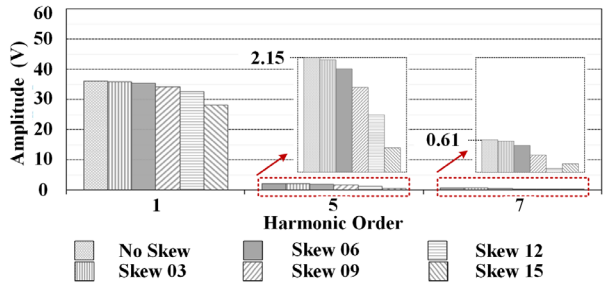

Fig. 6: Back EMF harmonics chart.

According to the harmonic back EMF simulation results shown in Fig. 6, the dominant harmonic values were observed at the 5th and 7th order harmonics. These higher-order harmonics can adversely affect the fundamental signal, potentially affecting the motor's performance and efficiency. Applying a stator skew angle of 6° showed a noticeable reduction in the magnitude of the 5th and 7th order harmonics. The value of the 5th order harmonic decreased from 2.15 to 1.93, and the 7th order harmonic value reduced from 0.60 to 0.50. This decrease in harmonic values is a positive outcome of implementing the 6° stator skew angle, which leads to a smoother and more trapezoidal back EMF waveform,[37].

4.4 Torque performance

Applying skew on stator BLDC motors reduces torque ripple, as shown in Fig. 7, whereby the motor torque graph got smoother as the stator skew angle increased[11]. At a 15° stator skew angle, the BLDC torque graph appeared stable without ripple torque. At a 6° stator skew angle, some torque ripple was still present, even though the torque graph exhibited improved smoothness and stability compared to a BLDC motor without a stator skew angle.

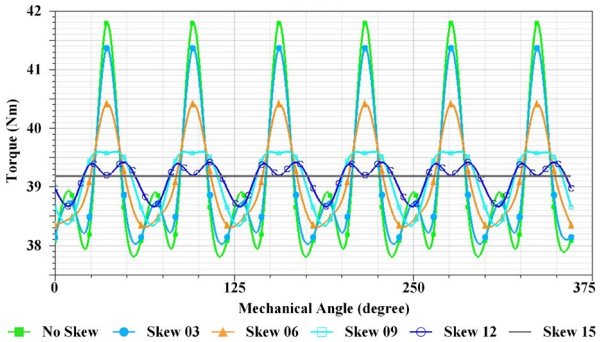

Fig. 7: Torque BLDC motor graphic.

By reducing the cogging torque in a BLDC motor, the quality of the output torque, the fundamental torque and its harmonics increased. Harmonics in the torque waveform typically occurred at specific orders, such as the 7th and 12th order. As the stator skew angle increased, the torque harmonics decreased. At a 6° skew angle, the harmonics at the 6th order reduced from 1.32705 Nm to 1.00052 Nm, while the harmonics at the 12th order decreased from 1.35578 Nm to 0.30248 Nm. This reduction in harmonics is attributed to a decrease in torque ripple experienced by the motor.

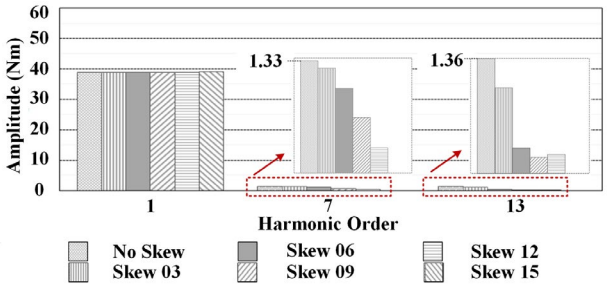

Fig. 8: Torque harmonics chart.

The simulation results in Table 5 provide a comprehensive view of the effects of varying the stator skew angle on the motor's performance. The table illustrates the impact of the stator skew angle on various parameters, including back EMF, total harmonic distortion (THD) of back EMF, torque ripple, cogging torque, and efficiency. The results indicated that applying stator skew angle variations offers advantages and disadvantages. One notable advantage is that skewing the stator core can significantly reduce cogging torque, leading to smoother motor operation. However, the influence of stator skew angle on other parameters should also be considered, such as back EMF, torque ripple, and efficiency. Based on Table 5, a 6° stator skew angle can be a good choice for reducing cogging torque while maintaining a high motor efficiency rating. At the stator skew angle of 6°, the back EMF, cogging torque, and torque ripple values are still within the tolerance limit, and the motor performance meets the good criteria.

Table 5. Motor performance in different skew angle

Parameter	Skew Angle						Unit
	0°	3°	6°	9°	12°	15°	
Back EMF	34.62	34.41	33.8	32,87	31,64	27,46	V
THD of Back EMF	6.242	6,106	5,677	4,753	3,308	1,738	%
Torque Ripple	9.3617	7,9319	5,2172	3,023	1,9553	0,04404	%
Cogging Torque	5.6615	4,3889	3,0196	1,8825	0,9195	0	Nm
Output Torque	38.2	38.2	38.2	38.2	38.2	38.2	Nm
Output Power	10	10	10	10	10	10	kW
Efficiency	94.545	94,51	94,399	94,195	93,887	92,823	%

4.5 Natural frequency

The type of modal analysis performed using the Mechanical ADPL solver is known as natural frequency

distribution analysis. This analysis involves creating finite element models (FEM) with three stator variations, namely stators with no skew, 6° skew angle, and 15° skew angle. These models are then compared to assess their respective characteristics. Fig. 9 shows the structural vibrations of the stator, shaft, and rotor, supported by bearings. The vibration model was simulated in 10 vibrations mode. The result of the simulation sample in 1st vibration mode showed that torsional stress in Z-axis started from the shaft tip to the bearing.

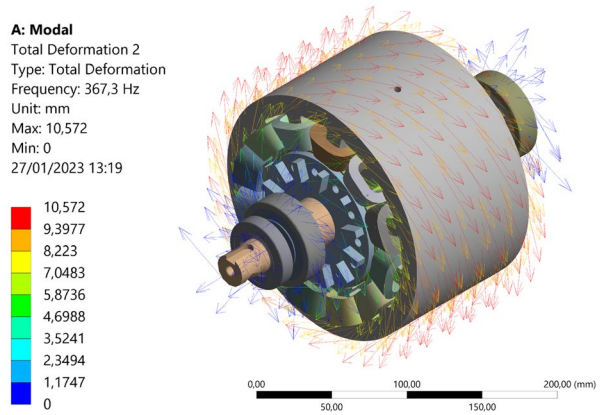

Fig. 9: Vibration mode vector direction 1 of 10 (torsional stress)

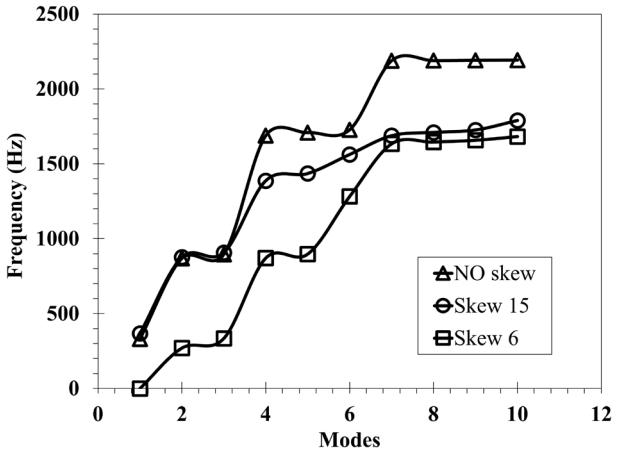

Fig. 10: Vibration mode of stator skewing

First, an analytical method was employed to examine the motor's structure and explain how it contributed to reducing cogging torque. Furthermore, to validate and further analyze the mechanical vibrations, finite element simulation analysis was conducted on two motor configurations using 6° and 15° skew angles. These specific skew angles were selected based on cogging torque analysis performed using ANSYS Maxwell.

In Fig. 10, the graph shows the natural frequencies in 10 vibration modes for three different motor configurations, namely no skew, 6° skew angle, and 15° skew angle. The first three vibration modes of all configurations tend to have the same frequency. However, from the 4th mode to the 10th mode, the no skew stator exhibited higher frequencies than the 15° skew angle configuration. The motor with a 6° skew angle showed lower frequencies than the 15° skew angle and the no skew configurations, starting from the 7th mode onwards. While the 6° skew angle led to higher cogging torque compared to the 15° skew angle, it displayed lower vibration levels. In summary, the findings from the natural frequency analysis indicated that a skew of 6° yields a favourable outcome in terms of mechanical/natural frequency analysis. This is attributed to the fact that the vibration level is significantly lower compared to a skew of 15°.

5. Conclusion

In conclusion, based on theoretical analysis and calculations, the optimal skew angle to reduce cogging torque for 12 stator slots and 8 poles BLDC motor was 15°. However, selecting this skew angle introduced manufacturing complexities and increased production costs. This research set a maximum limit of 10% of the rated torque for the cogging torque to find a balance between performance and manufacturing considerations. This led to selecting a stator skew angle of 6° as a compromise.

Simulation results confirmed that the 6° skew angle met the motor requirements. While it did not completely eliminate cogging torque and torque ripple, a vibration simulation revealed that the natural frequency of the motor with a 6° skew angle was lower than the optimal 15° skew angle. This suggested that the 6° skew angle was more suitable for performance and mechanical aspects.

It is important to note that the analysis and comparison presented in this research were based solely on software simulation results. Further testing of the overall motor performance was necessary to validate the effectiveness of the approach for determining the skew angle.

Acknowledgements

As a result, all authors, thank to Education Endowment Fund Management (LPDP) by Ministry of Finance Indonesia (grant No. PRJ-30/LPDP/2020) gave financial support for this research. Also, thank to Research Center of Process and Manufacturing Technology (PRTIPM) for supporting this research.

Nomenclature

Back EMF	Back electro-motive force.
BLDC	Brushless direct current motor.
CO_2	Carbon dioxide.
C_p	The least common multiple of the number of stator slots and the number of poles
E	Electro-motive force.
FEA	Finite element analysis.

HCF	The biggest common factor of number of poles and stator slot number
ICE	Internal combustion engine.
IPM	Interior permanent magnet.
K_{dk}	Distribution factor.
K_{pk}	Pitch factor.
K_{sk}	Skew factor.
$K_{sk\ /\ 2}$	Skew effect for flux in the kth tooth
Mechanical ADPL	Mechanical Ansys Parametric Design Language
N	Number of turns.
N_k	Turn per coil.
NO_x	Nitrogen oxide.
N_{period}	Cogging torque period in a single slot pitch
N_s	Number of stator slots.
N_t	The total number of turns per coil.
PM	Permanent magnet.
SPM	Surface permanent magnet.
T_{cog}	Cogging torque.
THD	Total harmonic distortion.
T_i	Harmonics
$T_{skew}(\theta)$	Torque on skew angle.
W	Magnetic energy.
α_{sk}	Skew angle.
θ_i	Phase angle.
θ_s	Angular slot pitch.
θ_m	Mechanical angle.
ϕ_i	Coefficients of the harmonic components.
$\phi(\theta)$	Tooth flux.
ω	Angular speed.
ϑ_r	Movable displacement part.
o	Degree.

References

1) A. Pal, K. Uddin, K. Thu, and B. Saha, "Environmental assessment and characteristics of next generation refrigerants," Evergreen, Joint Journal of Novel Carbon Resource Sciences & Green Asia Strategy, 5 (2) 58–66 (2018). doi:10.5109/1936218.
2) S. Sawant, R.M. Bin Raja Ahsan Shah, M. Rahman, A. Aziz, S. Smith, and A. Jumahat, "System modelling of an electric two-wheeled vehicle for energy management optimization study," Evergreen, 8 (3)642–650 (2021). doi:10.5109/4491656.
3) IEA, "Transport," Paris, 2022. https://www.iea.org/reports/transport (accessed January 30, 2023).
4) A. Habibie, M. Hisjam, W. Sutopo, and M. Nizam, "Sustainability evaluation of internal combustion engine motorcycle to electric motorcycle conversion," Evergreen, 8 (2) 469–476 (2021). doi:10.5109/4480731.
5) M.Z. Daud, K. Kin, J.S. Norbakyah, and S. Abdul Rahman, "An optimal electric machine control system design used in plug-in hybrid electric boat," ARPN Journal of Engineering and Applied Sciences, 10 (2015).
6) M.H. Huzaifi, M.A. Budiyanto, and S.J. Sirait, "Study on the carbon emission evaluation in a container port based on energy consumption data," Evergreen, 7 (1) 97–103 (2020). doi:10.5109/2740964.
7) S. Gómez-Oviedo, and R. Mejía-Gutiérrez, "An Interactive Tool For Propeller Selection According to Electric Motor Exploration: An Electric Boat Design Case Study," in: 2020 IEEE Transportation Electrification Conference & Expo (ITEC), 2020: pp. 147–151. doi:10.1109/ITEC48692.2020.9161467.
8) Y. Dönmezer, and L.T. Ergene, "Skewing effect on interior type BLDC motors," in: The XIX International Conference on Electrical Machines - ICEM 2010, 2010: pp. 1–5. doi:10.1109/ICELMACH.2010.5607848.
9) S. Leitner, H. Gruebler, and A. Muetze, "Cogging torque minimization and performance of the sub-fractional hp bldc claw-pole motor," IEEE Trans Ind Appl, 55 (5) 4653–4664 (2019). doi:10.1109/TIA.2019.2923569.
10) M. Jagiela, E.A. Mendrela, and P. Gottipati, "Investigation on a choice of stator slot skew angle in brushless pm machines," Electrical Engineering, 95 (3) 209–219 (2013). doi:10.1007/s00202-012-0252-8.
11) M.G. Angle, J.H. Lang, J.L. Kirtley, S. Kim, and D. Otten, "Cogging torque reduction in permanent-magnet synchronous machines with skew," in: 2016 XXII International Conference on Electrical Machines (ICEM), 2016: pp. 207–211. doi:10.1109/ICELMACH.2016.7732528.
12) Z. Shi, X. Sun, Y. Cai, Z. Yang, G. Lei, Y. Guo, and J. Zhu, "Torque analysis and dynamic performance improvement of a pmsm for evs by skew angle optimization," IEEE Transactions on Applied Superconductivity, 29 (2) 1–5 (2019). doi:10.1109/TASC.2018.2882419.
13) F.S. Bahrim, E. Sulaiman, R. Kumar, and L.I. Jusoh, "Cogging torque reduction techniques for spoke-type ipmsm," IOP Conf Ser Mater Sci Eng, 226 (1) 12128 (2017). doi:10.1088/1757-899X/226/1/012128.
14) Boldea, "Electric Generators Handbook - Two Volume Set," 2018. doi:10.1201/9781315214191.
15) R. Islam, and A.P. Ortega, "Practical aspects of implementing skew angle to reduce cogging torque for the mass-production of permanent magnet synchronous motors," in: 2017 20th International Conference on Electrical Machines and Systems (ICEMS), 2017: pp. 1–5. doi:10.1109/ICEMS.2017.8056084.

16) A.N. Patel, B.N. Suthar, T.H. Panchal, and R.M. Patel, "Comparative Performance Analysis of Radial Flux and Dual Air-Gap Axial Flux Permanent Magnet Brushless DC Motors for Electric Vehicle Application," in: 2018 2nd IEEE International Conference on Power Electronics, Intelligent Control and Energy Systems (ICPEICES), 2018: pp. 804–808. doi:10.1109/ICPEICES.2018.8897459.
17) R. Hiremath, "Finite element study of induced Emf, cogging torque and its reductions in BLDC motor," in: 2017 International Conference on Intelligent Computing, Instrumentation and Control Technologies (ICICICT), 2017: pp. 1665–1668. doi:10.1109/ICICICT1.2017.8342821.
18) A. Krings, and C. Monissen, "Review and trends in electric traction motors for battery electric and hybrid vehicles," in: Proceedings - 2020 International Conference on Electrical Machines, ICEM 2020, Institute of Electrical and Electronics Engineers Inc., 2020: pp. 1807–1813. doi:10.1109/ICEM49940.2020.9270946.
19) Safril, Mustofa, M. Zen, F. Sumasto, and M. Wirandi, "Design of cooling system on brushless dc motor to improve heat transfers efficiency," Evergreen, 9 (2) 584–593 (2022). doi:10.5109/4794206.
20) He, and T. Wu, "Design and Analysis of a V-type Fractional-Slots IPMSM with Distributed Winding for Electric Vehicles," n.d.
21) K. Yamazaki, M. Shina, Y. Kanou, M. Miwa, and J. Hagiwara, "Effect of eddy current loss reduction by segmentation of magnets in synchronous motors: difference between interior and surface types," IEEE Trans Magn, 45 (10) (2009). doi:10.1109/TMAG.2009.2024159.
22) B.-C. Kim, J.-H. Lee, and D.-W. Kang, "A study on the effect of eddy current loss and demagnetization characteristics of magnet division," IEEE Transactions on Applied Superconductivity, 30 (4) 1–5 (2020). doi:10.1109/TASC.2020.2986967.
23) Q. Chen, D. Liang, S. Jia, and X. Wan, "Analysis of multi-phase and multi-layer factional-slot concentrated-winding on pm eddy current loss considering axial segmentation and load operation," IEEE Trans Magn, PP 1–6 (2018). doi:10.1109/TMAG.2018.2841874.
24) R. Dutta, S. Sayeef, and M.F. Rahman, "Cogging Torque Analysis of a Segmented Interior Permanent Magnet Machine," n.d.
25) S. Duan, L. Zhou, and J. Wang, "Flux weakening mechanism of interior permanent magnet synchronous machines with segmented permanent magnets," IEEE TRANSACTIONS ON APPLIED SUPERCONDUCTIVITY, 24 (3) (2014). doi:10.1109/TASC.2013.2280847.
26) A. Gu, Y. Guo, J. Dong, B. Ruan, Y. Lian, S. Zhang, and X. Song, "Modeling and Analysis of the Flux-Weakening Range of Interior Permanent Magnet Synchronous Machines with Segmented Permanent Magnets," in: 2020 8th International Conference on Power Electronics Systems and Applications (PESA), 2020: pp. 1–6. doi:10.1109/PESA50370.2020.9343986.
27) Juha Pyrhonen, Tapani Jokinen, and Valeria Hrabovcova, "Design of Rotating Electrical Machines," 2nd Edition, Wiley, 2008. doi:10.1002/9780470740095.
28) E. Fleurot, F. Scuiller, and J.-F. Charpentier, "Analytical models for fast and accurate calculation of electromagnetic performances of segmented permanent magnet synchronous machines with large angular gaps," Applied Sciences, 11 (1) 459 (2021). doi:10.3390/app11010459.
29) Hanselman, "Brushless permanent magnet motor design," (2003).
30) L. Jia, M. Lin, W. Le, N. Li, and Y. Kong, "Dual-skew magnet for cogging torque minimization of axial flux pmsm with segmented stator," IEEE Trans Magn, 56 (2) 1–6 (2020). doi:10.1109/TMAG.2019.2951704.
31) S.-M. Hwang, J.-B. Eom, G.-B. Hwang, W.-B. Jeong, and Y.-H. Jung, "Cogging torque and acoustic noise reduction in permanent magnet motors by teeth pairing," IEEE Trans Magn, 36 (5) 3144–3146 (2000). doi:10.1109/20.908714.
32) M. Zhou, X. Zhang, W. Zhao, J. Ji, and J. Hu, "Influence of magnet shape on the cogging torque of a surface-mounted permanent magnet motor," Chinese Journal of Electrical Engineering, 5 40–50 (2019). doi:10.23919/CJEE.2019.000026.
33) M. Bao, E. Chen, Y. Lu, Z. Liu, and S. Liu, "Vibration and noise analysis for a motor of pure electric vehicle," Adv Mat Res, 915–916 98–102 (2014). doi:10.4028/www.scientific.net/AMR.915-916.98.
34) F. Ishibashi, M. Matsushita, S. Noda, and K. Tonoki, "Change of mechanical natural frequencies of induction motor," IEEE Trans Ind Appl, 46 (3) 922–927 (2010). doi:10.1109/TIA.2010.2046279.
35) X. Bao, C. Li, and C. Xiong, "Noise elimination algorithm for modal analysis," Appl Phys Lett, 107 41901 (2015). doi:10.1063/1.4927642.
36) T. Zhu, C. Zang, and Z. Genbei, "Noise reduction for modal parameter identification of the measured frfs using the modal peak-based hankel-svd method," Shock and Vibration, 2020 1–21 (2020). doi:10.1155/2020/8899189.
37) J. Wu, Y. Wang, X. Li, J. Zhang, and T. Wu, "Effect of parameters on back-EMF in permanent magnet brushless DC motor with concentrated winding," in: 2008 World Automation Congress, 2008: pp. 1–4.